*Manuscript published in Polymer, **120** (2017) 111-118.*

Model-free isoconversional method applied to polymer crystallization governed by the Hoffman-Lauritzen kinetics

Jordi Farjas[1], Joan Pere López-Olmedo[2] and Pere Roura[1]

[1]GRMT, Department of Physics, Campus Montilivi, Edif. P2, University of Girona, E17003-Girona, Catalonia (Spain)
[2]Unitat d'Anàlisi Tèrmica (STR), Campus Montilivi, Edif. P2, University of Girona, E17003-Girona, Catalonia (Spain)

*pere.roura@udg.cat, Tel. 34972418383, Fax. 34972418098

Abstract

A new method is developed to obtain the kinetic parameters of polymer crystallization from measurements of the transformation rate usually done at (but not restricted to) constant heating or cooling rates. It can be considered a generalization of the Fiedman's isoconversional method to deal with the Hoffman-Lauritzen temperature dependence. Apart from delivering the U* and Kg parameters as a function of the transformed fraction, this method allows to predict the crystallization course for an arbitrary thermal history. It has been applied to the crystallization of PET and PA6 samples, monitored by differential scanning calorimetry (DSC).

Keywords: crystallization; activation energy; calorimetry

I. Introduction

Polymer crystallization is a structural transformation that has an enormous influence on the quality of moulded thermoplastic components. Several critical properties such as optical transparency or yield strength [1] depend on the crystalline fraction, X_C. Furthermore, volumetric shrinking during crystallization has to be taken into account to ensure dimensional accuracy, and to avoid warpage when, as usual, processing involves highly non-homogeneous cooling conditions [2]. Consequently, reliable experimental methods to characterize crystallization kinetics as well as theoretical methods to analyze them and to apply the results to real processing conditions are needed.

Since the crystallization rate depends on temperature, isothermal experiments constitute the most straightforward approach to the phenomenon. Optical microscopy equipped with a hot stage is, probably, the technique that delivers the most accurate description because the nucleation, $\dot{N}$, and growth, G, rates of crystallites can be quantified independently [3]. Similar information can be obtained by light scattering [2,4,5]. From the $\dot{N}$ and G dependence on temperature, T, the evolution of the crystalline fraction can be predicted for isothermal and non-isothermal conditions. To this aim, a particular reaction model based on Avrami's equation is usually assumed [1, 2,3,6]. In any case, prediction of X_C evolution with time or temperature must be tested by a technique that, like differential scanning calorimetry (DSC), can directly quantify this evolution. Despite that deviations from the assumed kinetic model are usually encountered [1,6], predictions are satisfactory.

If one is interested in the evolution of crystallinity, it seems more reasonable to directly rely on DSC experiments for characterizing the crystallization kinetics. However, although isothermal DSC experiments can be done [1,6,7], this technique is more suitable for experiments performed at a constant rate of heating or cooling because these conditions allow exploring a much broader temperature range [2,8]. Experiments are much easier and faster to perform but their analysis requires application of specific kinetic methods. Among them, "isoconversional methods" are those that can be adapted to the broadest variety of structural transformations [9,10,11]. Most of them can be considered a generalization of the seminal Kissinger method [12]. They assume a number of restricting hypotheses. First of all, the "isoconversional principle" is assumed [13]; i.e. the reaction rate is taken as a function of temperature and transformed fraction, α, irrespectively of the thermal history:

$$\frac{d\alpha}{dt} = f(\alpha, T) \quad . \tag{1}$$

Second, an Arrhenian temperature dependence of the reaction rate is assumed:

$$\frac{d\alpha}{dt} = -k_\alpha(T)\cdot g(\alpha), \tag{2}$$

where $$k_\alpha(T) = k_{0\alpha} e^{-\frac{E_\alpha}{RT}} \tag{3}$$

and g(α) is characteristic of the "reaction model". In Eq.(3) E_α is the activation energy, R, the gas constant and $k_{0\alpha}$ the pre-exponential constant.

For E and k_0 independent of α, and constant heating rate

$$\beta = \frac{dT}{dt} \tag{4}$$

Eq.(2) has been integrated for many particular reaction models leading to analytic functions describing the peak shape of the transformation rate, $\dot{\alpha}(T)$ [14,15]. However, many solid state reactions are no so simple and their description requires allowing for the dependence of E and k_0 on α [16].

The variation of E with α is usually associated with complex reactions where the rate-controlling step switches from a low to a high activation energy step or vice versa (e.g. in crosslinking reactions [17] or in reactions that can be accomplished through two independent mechanisms acting in parallel [16]. Consequently, E_α and g(α) (in fact, $k_{0\alpha}\cdot g(\alpha)$) must be considered as phenomenological functions of α that allow to predict the reaction course for arbitrary thermal histories [18]. Under these circumstances E_α is referred as effective or apparent activation energy.

In general, description of the reaction rate by an Arrhenian dependence means that the process is limited by an energy barrier and, consequently, it goes faster at high temperature. However, when the equilibrium temperature, T^0, between the initial and final states is approached, an opposite temperature dependence appears because the reaction stops at T^0. Sometimes, like in solute precipitation from solid [19] or liquid [20] solutions or in solidification of pharmaceutical mixtures [21], an additional exponential term describes this dependence, e.g.:

$$k(T) = k_0 \exp\left(-\frac{E}{R(T-T_\infty)}\right)\cdot\exp\left(-\frac{Kf(T)}{(T^0-T)^2}\right) \quad , \tag{5}$$

where f(T) is a function that varies slowly around T^0. In Eq.(5), we have also considered the possibility of null molecular transport below T_∞.

Polymer crystallization follows this kind of temperature dependence. The growth rate of spherulites, G, is usually described by the Hoffman-Lauritzen (H-L) equation [22]:

$$k_{HL}(T) = k_0 \exp\left(-\frac{U^*}{T - T_\infty}\right) \cdot \exp\left(-\frac{Kg}{T \cdot \Delta T \cdot f}\right) \quad (6)$$

where $\Delta T \equiv T_m^0 - T$ (T_m^0, equilibrium melting temperature), $f \equiv \frac{2T}{T + T_m^0}$ and $T_\infty \approx T_g - 30$ (T_g, glass temperature). In Eq.(6), U* is the activation energy for chain diffusion and Kg is called the "nucleation constant". Although the H-L theory describes the growth rate, many authors assume the same dependency for the crystallization rate, k_{cryst}. However, in general, they will be different because k_{cryst} also depends on $\dot{N}$. For 3D spherulitic growth [23]:

$$k_{cryst} \propto (G^3 \dot{N})^{1/4}, \quad (7)$$

and, thanks to the larger contribution of G on k_{cryst}, the Kg and U* values obtained from k_{cryst} will be usually close to those of G.

Despite the great difference between the Arrhenian and the H-L dependencies, some authors have taken advantage of the flexibility of the isoconversional methods to deduce U* and Kg from a fictitious dependence of the activation energy (Eq.(3)) on temperature [17,24]. Since its proposal in 2004 by Vyazovkin and Sbirrazzuoli [24], this particular method has been applied by many authors to study the crystallization of a broad range of polymer materials such as pure polymers (e.g. refs.[25,26]), polymer blends (e.g. refs.[27,28]) and nanocomposites (e.g. refs. [29,30]) (a more complete review can be found in ref.[31]). This method assumes that the kinetic constants (U* and Kg) are independent of α. Consequently, the great advantage of the isoconversional methods to give full description of non-ideal processes (i.e. those whose parameters depend on α) is lost and prediction of the crystallization course is not possible.

Finally, many authors (see for instance refs.[1,6,27,32,33]) fit to Eq.(6) the temperature dependence of the time elapsed to reach α = 0.5 after the incubation period under isothermal conditions. This procedure is much simpler than that of Vyazovkin but it also assumes that Kg and U* are independent of α.

The present paper describes the crystallization course of polymers assuming the dependence on α of Eq.(1) but without the need to suppose that the reaction rate constant has an Arrhenian dependence on temperature (Eq.(3)). After a brief description of the experiments (Section II), the proposed method of analysis will be explained (Section III) and

tested against crystallization experiments on two polymers (PET and PA6) (section IV and VI). The paper will continue with a brief discussion and a concluding section.

II. Experimental

Pure PET and PA6 samples were used for this study. Number-average molecular weight of both polymers was determined using solution viscosity measurements and Mark-Houwink equation. The values obtained were 36.400 g/mol for PET and 19.000 g/mol for PA6.

The crystallization course of the PET and PA6 samples has been measured by DSC (Q2000 apparatus of TA instruments). Samples were put inside aluminium pans and protected during the DSC experiments by an inert atmosphere of N_2 (100 mL/min). Melt crystallization was studied by cooling down at several controlled rates beginning at a temperature (280ºC and 250ºC for PET and PA6, respectively) above the maximum temperature of the sample's DSC melting peak. To minimize thermal degradation, no isothermal period was programmed before cooling. For glass crystallization experiments, the samples were quenched into liquid nitrogen and heated at a controlled heating rate up to the melting temperature. Comparison between the heat of crystallization, Q_{cryst}, and the heat of melting, Q_m, was used to assess if a fully amorphous state was reached after quenching. For PA6 samples, it was impossible to reach it (after quenching $Q_{cryst} \cong Q_m/3$) and, consequently, its glass crystallization kinetics was not studied. The difficulty to reach 10% amorphous PA6 by quenching from the melt is consistent with the literature. With a cooling rate as fast as 450ºC/s, X_C is still above 6% [34]. We estimate that during quenching in liquid nitrogen we reached 150ºC/s.

Thanks to the physical construction of our DSC cell, it was possible to measure the temperature of the sample during all the experiments, and no significant deviations from the programmed temperature history were detected. However, heat transport inside a low thermal diffusivity material like a polymer produces temperature gradients inside the sample. We have corrected the temperature of all the DSC peaks by a constant value corresponding to the average sample overheating arising from both the inertial term [35,36]:

$$\overline{\Delta T_{cp}} = -\frac{1}{2}\frac{\beta}{D}h^2, \qquad (8)$$

where D is thermal diffusivity ($1.8\cdot10^{-7}$ and $1.0\cdot10^{-7}$ m^2/s for PET and PA6, respectively) and h is the sample thickness (0.4 and 1 mm, for the PET and PA6 samples), and from the heat of crystallization [35]:

$$\overline{\Delta T_Q} = \frac{1}{2}\frac{h}{A}\frac{\dot{Q}_{MAX}}{\kappa}, \qquad (9)$$

where A is the sample contact area with the pan (0.2 and 0.1 cm^2 for PET and PA6)[37], κ, thermal conductivity (0.29 W/(m·K) for PET and, also, for PA6) and Q_{MAX} the heat evolved per unit time at the DSC peak maximum. Due to its higher thickness, h, and smaller section, A, these corrections were only significant for the experiments on PA6. At the highest cooling rate (-40 K/min), $\overline{\Delta T_{cp}}$ = 1.6ºC and $\overline{\Delta T_Q}$ = 0.7ºC.

III. Description of the isoconversional method

Notice that the H-L equation has two exponential factors whose dependencies on temperature are oposed. Whereas the exponential factor with U* continuously grows from zero at $T = T_\infty$ when temperature is increased, the factor with Kg diminishes down to zero when temperature is increased until T_m^0 is reached. Consequently, crystallization can be done by cooling down from T_m^0 (melt crystallization) or by heating up from T_∞ (glass crystallization). Obviously, the simplest experiments are those carried isothermally or at constant heating or cooling rates.

The crystallization kinetics will be fully described when the free parameters, U*, Kg, and k_0 together with the reaction model, g(α), are determined. Let all of them vary with α; i.e. U_α*, Kg_α and $k_{0\alpha}$·g(α). From Eq. (1) and assuming that the rate constant is given by Eq.(6), the crystallization rate can be written as:

$$\dot{\alpha}(t,T) = k_{HL\alpha}(T)\cdot g(\alpha(t,T)). \qquad (10)$$

Let us consider that a given value of α is attained through several experiments performed at different constant heating or cooling rates, β_i. Given that the sample will follow different thermal histories, $\dot{\alpha}_i$ will be different for each one. In any case, it will obey Eq.(10), now transformed into:

$$\dot{\alpha}_i = k_{0\alpha}\cdot g(\alpha)\exp\left(-\frac{U_\alpha^*}{T_i - T_\infty}\right)\exp\left(-\frac{Kg_\alpha}{T_i\cdot\Delta T_i\cdot f_i}\right). \qquad (11)$$

where $\dot{\alpha}_i \equiv \dot{\alpha}(t_i, T_i)$. Eq.(11) constitutes a system of non-linear equations on U_α* an Kg_α and $k_{0\alpha}g(\alpha)$. Thanks to the particular dependence on U_α* and Kg_α, the unknowns can be obtained after the iterative sequence of linear fittings described below.

Consider that you have done several experiments of melt and glass crystallization. Since, on cooling, crystallization occurs nearer to T_m^0 than to T_∞, the corresponding $\dot{\alpha}_i$ values are mainly governed by Kg_α whereas they are weakly dependent on U_α^*. The contrary holds for crystallization during heating, because it occurs closer to T_∞ than to T_m^0 (Fig.1).

Now, take a realistic guess value for U_α^*.This allows for Eq.(11) to be linearized:

$$\ln(\dot{\alpha}_i) + \frac{U_\alpha^*}{T_i - T_\infty} = \ln[k_{0\alpha} \cdot g(\alpha)] - \frac{Kg_\alpha}{T_i \cdot \Delta T_i \cdot f_i}, \tag{12}$$

and to obtain $k_{0\alpha} \cdot g(\alpha)$ and Kg_α by linear fitting of $Y_i \equiv \ln(-\dot{\alpha}_i) + \frac{U_\alpha^*}{T_i - T_\infty}$ vs $X_i \equiv \frac{1}{T_i \cdot \Delta T_i \cdot f_i}$ (the "U*-plot"). Of course, since the guess value of U_α^* is not the solution, the experimental points will not be very well aligned and a second linear fitting (Kg-plot) will be done to obtain U_α^* from the equation:

$$\ln(-\dot{\alpha}_i) + \frac{Kg_\alpha}{T_i \cdot \Delta T_i \cdot f_i} = \ln[k_{0\alpha} \cdot g(\alpha)] - \frac{U_\alpha^*}{T_i - T_\infty}, \tag{13}$$

where Kg_α is the value obtained in the former fitting.

The U-plot has been extensively used for isothermal crystallization experiments measuring G or the crystallization half-time since the days when Hofmann and Lauritzen proposed its kinetics. The alternate fittings from U-plot to the Kg-plot we propose ensure a similar "weight" of melt and glass crystallization experiments in the final U_α^* and Kg_α values. If the experiments cover the two temperature ranges where either U_α^* or Kg_α dominate the temperature dependence, the procedure converges to a constant value of U_α^* and Kg_α.

For the particular case of PET crystallization and $\alpha = 0.5$ (Fig.2), convergence has been reached after 42 iterations. In this case, the final R-square correlation coefficients are very close to one (0.9979 and 0.9972) and the relative standard error of U_α^* and Kg_α deduced from the last fitting is ±2%. However, the real uncertainty is higher. The $\ln(\dot{\alpha}_i)$ vs T_i points have also been fitted by a non-linear procedure. The Kg and U* values coincide with those of the iterative method but with larger error bars of ±7%. This apparent discrepancy together with a hint of how to simplify the iterative procedure is explained in Appendix A.

IV. Crystallization of PET

Melt and glass crystallization experiments were done on thin (0.7 mm approx.) PET specimens of mass around 4 mg. The crystallization heat of the melt diminished steadily from the lowest (48.4 J/g at -1.25 K/min) to the fastest (46.0 J/g at -20 K/min) cooling experiments. During the heating experiments ($2.5 < \beta < 20$ K/min), Q_{cryst} was smaller (42±1 J/g). These values should be compared to the heat of melting of 100% crystalline PET (ΔH_f = 140 J/g [38]). The difference means that the final state reached with our experiments has a crystallinity below 50%. All the DSC peaks have a queue at long times that could correspond to a secondary crystallization process, similar to that reported by other authors [1,7]. Notice in Fig.3 (and in the upper part of Fig.1), that this process is more important during glass crystallization.

Application of the method described in the previous section, with T_∞ = 312 K [17] and T_m^0 = 553 K [1], has delivered the dependence on α of Kg, U* and $k_0 \cdot g(\alpha)$ shown by the solid curves of Fig.4. Whereas Kg is nearly constant from α = 0.1 to 0.8, U* increases steadily. The U* value at α = 0.9 almost triplicates the value at 0.1 (6000 J/mol). Since, in principle, one expects G to be independent of α (laser scattering [2] and transmission electron microscopy [39] have shown linear growth until impingement) this variation is surprising. A simple explanation arises if we consider that the long queue of the DSC peaks correspond to an independent crystallization process. In fact, it has been shown that, when crystallization occurs through two parallel processes, the activation energy determined by isoconversional methods exhibits a fictitious increment with α [16].

To analyze the main crystallization process (the one occurring first) we take into account that, at the peak temperature, $\alpha \equiv \alpha_{MAX} = 0.5$ for melt crystallization. In contrast, for glass crystallization, α_{MAX} is much smaller and depends on the particular experiment (α_{MAX} = 0.33 – 0.39). We thus make the hypothesis that, at the peak maximum, the degree of completion of the first crystallization process, α_1, is always the same and equal to 0.5. So, we define:

$$\alpha_1 \equiv \alpha \frac{0.5}{\alpha_{MAX}} , \qquad (14)$$

and we renormalize the crystallization rate, $\dot{\alpha}_1$, accordingly. We have applied the fitting method of Section III to obtain Kg_α, U_α* and $k_{0\alpha} \cdot g(\alpha)$ for discrete values of α_1. Calculations have ended at α_1 = 0.8 (α = 0.52 - 0.62 for glass crystallization and 0.8 for melt crystallization) to avoid a significant contribution of the secondary process. The result has been added in Fig.4 as full symbols.

Now U* is nearly constant (7.3-8.2 kJ/mol) as expected, and Kg increases only slightly with α ($4.7 \cdot 10^5$ to $5.9 \cdot 10^5$ K^2). An additional proof for the correctness of these values compared to those obtained above comes from error analysis; the error bars of U* shown in Fig.4c correspond to the solid line. This means that, before renormalization of α into α_1, the points of the Kg-plot were not very well aligned (notably for $\alpha_1 > 0.5$), indicating that the overall crystallization process does not follow the H-L kinetics.

Our Kg and U* values fall within the wide range reported in the literature (Table I). Notice that, in Table I, the Kg values obtained from measurements of G [2,5,39,40] are, on the average, lower than those obtained from the crystallization rate. This is not strange because, since $\dot{N}$ grows as the temperature departs from T_m^0, it will also contribute to the fitted value coming from the crystallization rate (Eq.7). The higher Kg value corresponds to a faster increase of $\dot{N}$ with respect G when temperature diminishes below T_m^0. This is what occurs in ref.[2] where the density of crystallites grows steadily by 5 orders of magnitude from 220 to 130ºC.

We can determine the crystallization regime from the Kg value after applying the Lauritzen Z-test [41]. In regime I nuclei grow so fast that formation of any nucleus is followed by rapid completion of the substrate whereas, in regime II, nuclei grow slowly and many nuclei form before substrate completion. The lamellar width, L, is related to the so-called Z-parameter according to:

$$L \approx 2a_0\left(\frac{Z}{10^3}\right)^{1/2} \exp\frac{4Kg}{nT\cdot\Delta T} \quad , \qquad (15)$$

where a_0 is the width of the molecular chain in the crystal (around 0.5 nm), and $Z \leq 0.01$ or ≤ 1.0, and n = 4 or n = 2 for regimes I or II, respectively [41]. A realistic value for the lamella width (L < 34 nm) is only obtained for regime I that applies to the whole temperature range of our experiments (notice that all points are aligned in the U- and Kg plot of Fig.2). Once the crystallization regime is known, the product of the lateral energy times the fold surface energy, $\sigma\sigma_e$, can be calculated through [22]:

$$\sigma\sigma_e = \frac{Kg\Delta h_f k_B}{nbT_m^0}, \qquad (16)$$

where k_B is the Bolzmann constant, Δh_f, the melting enthalpy of the perfect crystal per unit volume ($\Delta h_f = \Delta H_f \cdot \rho_c = 210$ J/cm^3 for PET whose crystal density is $\rho_c = 1.5$ g/cm^3) and b, the

monolayer thickness (0.553 nm [24]). We obtain, $\sigma\sigma_e = 12\ 10^{-4}\ J^2m^{-4}$, that is similar to the values published by most authors [24].

Before leaving this section, we will check the goodness of our analysis by using the Kg_α, U_α^* and $k_{0\alpha}{\cdot}g(\alpha)$ values to calculate the overall crystallization rate ($d\alpha/dt$) and compare it to the experimental DSC peaks. Eq.(2) has been numerically integrated following the method of Farjas developed in refs. [18,42], with the especial condition that crystallization begins after an incubation period. For crystallization experiments performed during cooling or heating ramps, this condition corresponds to $d\alpha/dt = 0$ until $T = T_{ONSET}$ [2], where T_{ONSET} is the experimental onset temperature of the DSC peak. In Fig.3, the calculated and experimental peaks are compared. There is good agreement despite that, as discussed above, the overall crystallization of our samples is a complex transformation that involves two individual processes. In fact, the discrepancies seen in Fig.3 mainly arise from the experiment (the DSC peaks do not have a steady evolution when the heating or cooling rate is changed).

Although the long queue of the DSC peaks makes that the isoconversional principle is not fully obeyed in this experiments of PET crystallization, this example constitutes an additional proof [10,11,18,42, 43] of the flexibility of model-free isoconversional methods to predict the course of complex transformations.

V. Crystallization of PA6

The experiments on PA6 were done on single pellets ($m \cong 10$ mg). Since quenching in liquid nitrogen didn't gave a 100% amorphous state, the reported results are those of melt crystallization ($3.5 < |\beta| < 40$ K/min). As the cooling rate increased, Q_{cryst} steadily decreased from 53 to 38 J/g indicating a higher difficulty to crystallize. Again, like with PET, Q_{cryst} is much smaller than the enthalpy of full crystallization ($\Delta H_f = 190$ J/g [44]).

Once the DSC peaks have been shifted to correct for the sample thermal lag (Section II) and, in view of their long queue, we have subtracted this secondary crystallization process as shown in Fig.5. Then, the equilibrium melting temperature, T_m^0, has been determined by the Hoffmann-Weeks method [45]. We have obtained $T_m^0 = 222$ºC. This value and $T_\infty = 20$ºC have been used as input parameters to apply the iterative method described in Section III to obtain the crystallization kinetic parameters of PA6. The result is shown in Fig.6. Kg is almost constant ($1.02\pm0.05\ 10^5\ K^2$ for $0.05 < \alpha < 0.95$, whereas the U* dependence on α has a peak below $\alpha = 0.3$. Above $\alpha = 0.3$, $U^* = 3.1\pm0.2$ kJ/mol. Probably, the peak of U* is related

to the initial faster crystallization (high temperature side of DSC peaks) seen on the DSC peaks (Figs.5 and 7).

Our Kg value falls on the lower range of the reported values obtained from DSC experiments [46, 47, 32, 33, 26] or from direct measurement of G [48], and our U* value is closer to that extracted from G (4.0 kJ/mol) than that from non-isothermal DSC (3.3 kJ/mol [26]) (see Table II). However, without crystallization experiments at temperatures closer to T_∞ than to T_m^0, one cannot be very confident on the fitted value of U*. As with PET, most Kg values of PA6 obtained from DSC are higher than that obtained from G. For PA6, the Lauritzen Z-test tells us that crystallization occurs in regime II, and application of Eq.(16) (n = 2, b = 1.9 nm, ρ_c = 1.24 g/cm^3, Δh_f = 236 J/cm^3[46]) delivers $\sigma\sigma_e$ = 17 10^{-5} J^2/m^4.

The kinetic parameters of Fig.6 together with the T_{ONSET} values (inset of Fig.5) allow us to calculate the melt crystallization rate during arbitrary thermal histories. Agreement with experiment is excellent when the experiments carried out at a constant cooling rate are simulated (Fig.7). Two further tests on the predictive capability have been done by cooling the melt at -20 K/min down to an isothermal stage (at 190ºC and 180ºC). The predicted transformation rates are compared with the DSC experiments in Fig.8. They show good agreement. Since at -20 K/min T_{ONSET} = 83.7ºC, crystallization begins during the cooling period before the isotherm (inset of Fig.8). This short period has an influence on the crystallization course as illustrated by the comparison between the curves predicted with or without cooling ramp. As expected, the best agreement with experiments is achieved in the first case (Fig.8). Concerning the isotherm at 190ºC, crystallization begins after an initial incubation time that, from the T_{ONSET} values (inset of Fig.5) has been estimated to be 30 s, following the method of ref. [49]. In view of the long crystallization time at this temperature (Fig. 8), the incubation period is too short to be relevant.

VI. Conclusions and perspectives

In this paper, we have developed a new isoconversional method to obtain the kinetic parameters of Hoffman-Lauritzen model (U* and Kg) governing polymer crystallization. It involves an iterative procedure to optimize the linear fits of modified Friedman's plots [50] and can be applied to experiments carried out at any thermal conditions (constant or varying heating rates and isothermal). Compared with the current methods to obtain U* and Kg (fit to the isothermal crystallization half-time, and Vyazovkin's method for non-isothermal experiments [17]), these parameters are allowed to vary with the crystalline fraction, α. In

case they are constant, the fitting procedure needs to be applied to a single value of α only and, as shown in Appendix A, becomes as simple as with the current methods.

It has been applied to analyse the DSC crystallization curves of PET and PA6 samples. Since PET crystallization has been done from the melt and from the glass states, accurate values of U* and Kg have been obtained as a function of α. In a preliminary analysis, U* remained constant around 7.5 kJ/mol up to a transformed fraction of 0.5 and, then, it increased steadily. It has been shown that this anomalous variation was fictitious because it disappeared when the secondary crystallization occurring at long times was subtracted from the DSC signal. Kg was much less sensitive to the secondary crystallization and remained almost constant around $5.3 \cdot 10^5$ K^2.

In contrast with PET, PA6 crystallization could only be done from the melt and, consequently, the fitted value of U* was less reliable than that of Kg. Kg remained almost constant around $1.0 \cdot 10^5$ K^2 whereas U* showed a peak below $\alpha = 0.3$ that has been attributed to a faster initial crystallization rate.

In addition to extracting the kinetic parameters, our method allows to predict the crystallization course for an arbitrary thermal history. This possibility has been tested by comparing the DSC curves measured at several heating and cooling rates with the predicted curves. Moreover, isothermal crystallization of PA6 after a cooling ramp has been successfully simulated.

To the best of our knowledge, this is the first time that an isoconversional method is able to obtain the dependence of the kinetic parameters on the transformed fraction and to make predictions of the crystallization course for a process that follows a temperature dependence as complex as that of Hoffman-Lauritzen (the easier case of crystallization just below the melting point was already done in ref.[51]). It opens the door to the analysis of a broader range of polymers and processes with temperature dependencies similar to that of Hoffman-Lauritzen, like those already commented on in the Introduction. Furthermore, even those processes not having well-established temperature dependence such as sol-gel transformation of gelatin [52] or collagen denaturation [53], but occurring near equilibrium, are also candidates for this kind of analysis.

Acknowledgments

This work was funded by the Spanish Programa Nacional de Materiales through project MAT2014-51778-C2-2-R. We also acknowledge financial support from the Generalitat de

Catalunya (contract num.SGR948) and from the University of Girona (program MPCUdG2016).

Appendix A

Fig.A1 collects several Kg (U*) points obtained from fitting the U-plot (Kg-plot) of PET for $\alpha = 0.5$ for several guess values of U* (Kg). The intersection of both series of points is the solution delivered by our iterative procedure and is indicated by a full square with solid error bars. The meaning of these error bars is the standard error of Kg when U* is fixed and viceversa.

Alternatively, U* and Kg can be obtained by non-linear fitting of the $\ln(\dot{\alpha}_i)$ vs T_i plot to the H-L dependence (Fig.A2). The result coincides with that of the previous procedure (filled square in Fig A.1) but with larger error bars (dashed in Fig.A1). These bars correspond to the projection to the Kg and U* axes of the ellipse of (Kg,U*) values with 68% confidence level (also drawn in Fig.A1) whereas the error bars of the iterative procedure are the vertical and horizontal sections of the ellipse. Since the fitted values of Kg and U* are not independent, the correct error bars are those given by the non-linear fitting [55].

References

[1] X.F. Lu and J.N.Hay, Polymer **42** (2001) 9423-9431.

[2] M.Okamoto, Y.Shinoda, N.Kinami, T.Okuyama, Appl.Pol.Sci. **57** (1995) 155-1061.

[3] J.-M. Huang, F.Ch.Chang, J.Polym.Sci.B: Polym.Phys. **38** (2000) 934-941.

[4] R.S.Stein, M.B.Rhodes, J.Appl.Phys. **31** (1960) 1873.

[5] P.J.Phillips, H.T.Tseng, Macromol.**22** (1989) 1649-1655.

[6] T.W. Chan, I.Isayev, Polym.Eng.Sci. **34** (1994) 461-471.

[7] S.Vyazovkin, N.Sbirrazzuoli, J.Phys.Chem.B **107** (203) 882-888.

[8] S. Vyazovkin, A.K. Burnham, J.M. Criado, L.A. Pérez-maqueda, C. Popescu, N. Sbirrazzuoli, Thermochim. Acta. **520** (2011) 1–19.

[9] J.Farjas, P.Roura, J.Therm.Anal.Calorim. **105** (2011) 757-766.

[10] Brown ME, Maciejewski M, Vyazovkin S, Nomen R, Sempere J, Burnham A, Opfermann J, Strey R, Anderson HL, Kemmler A, Keuleers R, Janssens J, Desseyn HO, Li CR, Tang TB, Roduit B, Malek J, Mitsuhashi T. Thermochim Acta. **355** (2000) 125–43.

[11] A. Khawam, D.R. Flanagan, J. Pharm. Sci. **95** (2006) 472–98.

[12] H.E. Kissinger, Anal. Chem. **29** (1957) 1702–1706.

[13] Vyazovkin S, J Comput Chem. **18** (1997) 393–402.

[14] J.Farjas, P.Roura, AICHE J. **54** (2008) 2145-2154.

[15] J. Farjas, N. Butchosa, P. Roura, J. Therm. Anal. Calorim. **102** (2010) 615–625.

[16] J.Farjas, P.Roura, J.Therm.Anal.Calorim. **105** (2011) 767-773.

[17] S.Vyazovkin, N.Sbirrazzuoli, Macromol.Rapid.Comm. **27** (2006) 1515-1532.

[18] J.Farjas, P.Roura, J.Therm.Anal.Calorim. **109** (2012) 183-191.

[19] I.S.Servi and D.Turnbull, Acta.Met. **14** (1966) 161-169.

[20] V.L.Stanford, C.M.McCulley and S.Vyazovkin, J.Phys.Chem.B **20** (2016) 5703-5709.

[21] N.Clavaguera, J.Saurina, J.Lheritier, J.Masse, A.Chauvet, M.T.Clavaguera-Mora, Termochim.Acta **290** (1997) 173-180.

[22] J.D.Hoffman, J.I.Lauritzen, J.Res.Natl.Bur.Stand, (A) **65** (1961) 279.

[23] J.Farjas and P.Roura, Acta Mater., **54** (2006) 5573-5579.

[24] S.Vyazovkin, N.Sbirrazzuoli, Macromol.Rapid.Comm. **25** (2004) 733-738.

[25] N.Bosq, N.Guigo, E.Zhulavlev, N.Sbirrazzuoli, J.Phys.Chem.B **117** (2013) 3407.

[26] D.S.Achilias, G.Z.Papageorgiou, G.P.Karayannidis, Macromol.Chem.Phys. **206** (2005) 1511.

[27] J.-W.Huang, Ch.-Ch.Chang, Ch.-Ch.Kang and M.-Y.Yeh, Thermochim.Acta **468** (2008) 66-74.

[28] A.Roy, B.Dutta, S.Bhattacharya, J.Matter.Sci. **51** (2016) 7814.
[29] B.Guo, Q.Zou, Y.Lei, M.Du, M.Liu and D.Jia, Thermochim.Acta **484** (2009) 48-56.
[30] S.P.Lonkar, S.Morlat-Therias, N.Capera, F.Leroux, J.L.Gardette, R.P.Singh, Polymer **50** (2009) 1505.
[31] S.Vyazovkin, Macromol.Rapid.Comm. **38** (2017) 1600615.
[32] S.Sanh, A.Durmus and N.Ercan, J.Mater.Sci. **47** (2012) 3052-3063.
[33] J.Li, Z.Fang, Y.Zhu, L.Tong, A.Gu and F.Liu, J.Appl.Polym.Sci. **105** (2007) 3531-3542.
[34] V.Brucato, Polym.Eng.Sci. **31** (1991) 1411-1416.
[35] D.Sanchez-Rodriguez, H. Eloussifi, J. Farjas, P. Roura and M. Dammak, Thermochim.Acta **589** (2014) 37-46.
[36] P. Holba, J. Šesták, D. Sedmidubský, Heat Transfer and Phase Transition in DTA Experiments, in: J. Šesták, P. Šimon (Eds.), Therm. Anal. Micro, Nano- Non-Crystalline Mater., Springer Netherlands, 2013: pp. 99–133.
[37] H.Domininghaus, Plastics for Engineers, 2nd. Ed., Hanser, Munich, 1988.
[38] B.Wunderlich, Macromolecular Physics, vol.3, Academic Press, New York, 1980.
[39] L.H.Palys, P.J.Phillips, J.Polym.Sci: Polym.Phys. **18** (1980) 892-852.
[40] F.Van Antwerpen and D.W.van Krevelen, J.Polym.Sci: Polym.Phys.Ed. **10** (1972) 2423.
[41] J.I.Lauritzen and J.D.Hoffman, J.Appl.Phys. **44** (1973) 4340.
[42] H. Eloussifi, J. Farjas, P. Roura, M. Dammak, J. Therm. Anal. Calorim. **108** (2012) 597–603.
[43] A.Perez, J.P.Lopez-Olmedo, J.Farjas, P.Roura, J.Therm.Anal.Calorim. **125** (2016) 667–672.
[44] I.Campoy, M.A.Gomez and C.Marco, Polymer **39** (1988) 6279.
[45] J.D.Hoffman and J.J.Weeks, J.Res.Nat.Bur.Stand. **66A** (1962) 13.
[46] T.M.Wu, Y.H.Lien and S.F.Hsu, J.Appl.Polym.Sci. **94** (2004) 2196.
[47] W.Weng, G.Chen and D.Wu, Polymer **44** (2003) 8119.
[48] B.B.Burnett, and W.F.McDevit, J.Appl.Phys. **28** (1957) 1101.
[49] W.L.Sifleet, N.Dinos and J.R.Collier, Polym.Eng.Sci. **13** (1973) 10.
[50] H.L.Friedman, J.Polym.Sci.C **6** (1964) 183-195.
[51] R.Berlanga, J.Farjas, J.Saurina and J.J.Suñol, J.Therm.Anal.Calorim. **52** (1988) 765-772.
[52] K.Chen and S.Vyazovkin, Macromol.Biosci. **9** (2009) 383-392.
[53] S.Vyazovkin, L.Vincent and N.Sbirrazzuoli, Macromol.Biosci. **7** (2007) 1181-1186.
[54] M.H.Rahman and A.K.Nandi, Polymer **203** (2002) 653-662.

[55] W.H. Press, S.A.Teukolsky,W.T.Vetterling, B.P.Flannery, Numerical Recipes 3rd edition The Art of Scientific Computing, Cambridge University Press, New York, 2007.
[56] J.Runt, D.M.Miley, X.Zhang, K.P.Gallagher, K.McFeaters and J.Fishburn, Polymer **25** (1992) 1929-1934.

Table I.- Kinetic parameters of PET crystallization

From measurements of G		
Kg (10^5 K^2)	U* (kJ/mol)	references
2.4	5.8	Okamoto et al. [2]
4.14	8.1	Phillips et al. [5]&
2.92	6.45	Palys et al. [39]
2.8-3.2	6.3	van Antwerpen [40]%
From measurements of the crystallization rate		
Kg (10^5 K^2)	U* (kJ/mol)	references
4.6	6.4	Lu et al. [1]$
6.1	--	Rahman et al. [54] $
3.7	6.3	Chan et al. [6]
3.4	7.5	Phillips et al. [5]&
3.2	4.3	Vyazovkin et al. [7]

& G(T) dependence fitted by us.
% G(T) dependence fitted by Runt et al. [56]. Kg varied with molecular weight.
$ The "universal" value of U* (6.3 kJ/mol) was assumed.

Table II.- Kinetic parameters of PA6 crystallization

From measurements of G		
Kg (10^5 K^2)	U* (kJ/mol)	references
1.17	4.0	Burnett et al. [48]&
From measurements of the crystallization rate		
Kg (10^5 K^2)	U* (kJ/mol)	references
0.74	--	Wu et al. [46]%
1.53	--	Weng et al. [47] %
1.81	--	Sanh et al. [32] %
1.63	--	Li et al. [33] %
1.08	--	Huang et al. [27] %
1.09-1.17, 1.32	--, 7.3	Huang et al. [27]$
2.33	6.2	Guo et al. [29]$

& G(T) dependence fitted by us.
% Isothermal DSC. The "universal" value of U* (6.3 kJ/mol) was assumed.
$ Non-isothermal DSC. In ref.[27] results depend on the fitting method.

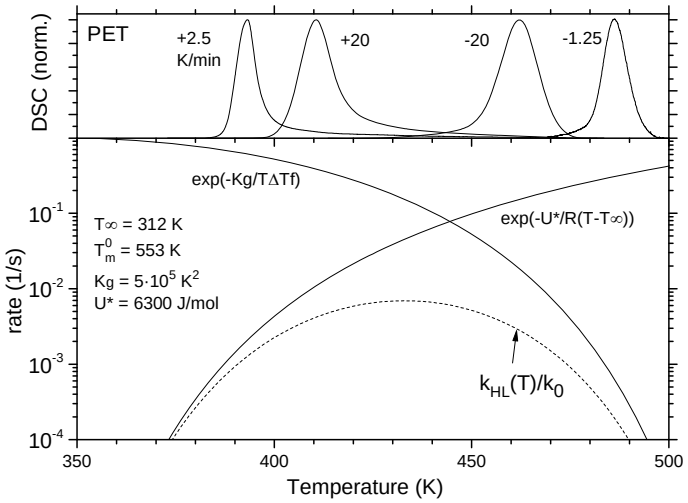

Figure 1.- The contribution of the Kg and U* terms to the Hoffman-Lauritzen kinetic constant. The U* term alone almost determines the kinetics of glass crystallization (+2.5 and +20 K/min DSC peaks) whereas the Kg term, that of melt crystallization (-20 and -1.25 K/min peaks).

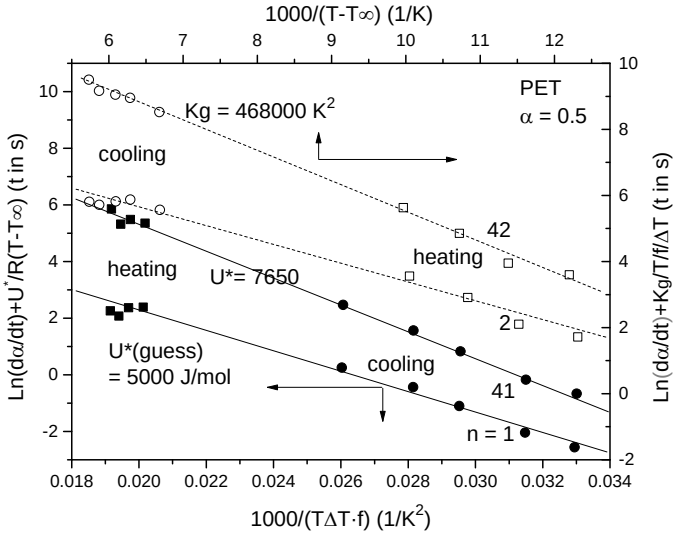

Figure 2.- Initial and last fittings (n gives their order) of the iterative procedure used to determine the values of U* and Kg. Kg is proportional to the slope of the U-plot (bottom-left axes), and U*, to that of the Kg-plot (top-right axes).

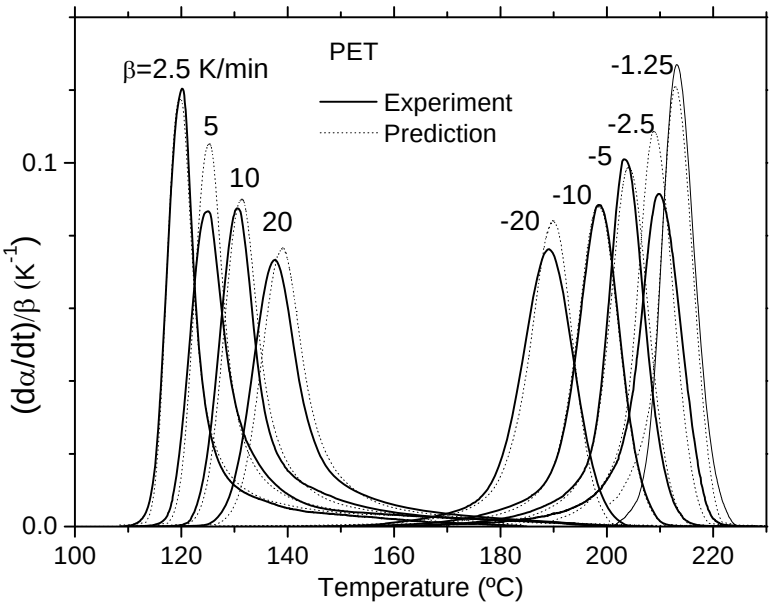

Figure 3.- Transformation rates of glass and melt crystallization of PET at different heating and cooling rates.

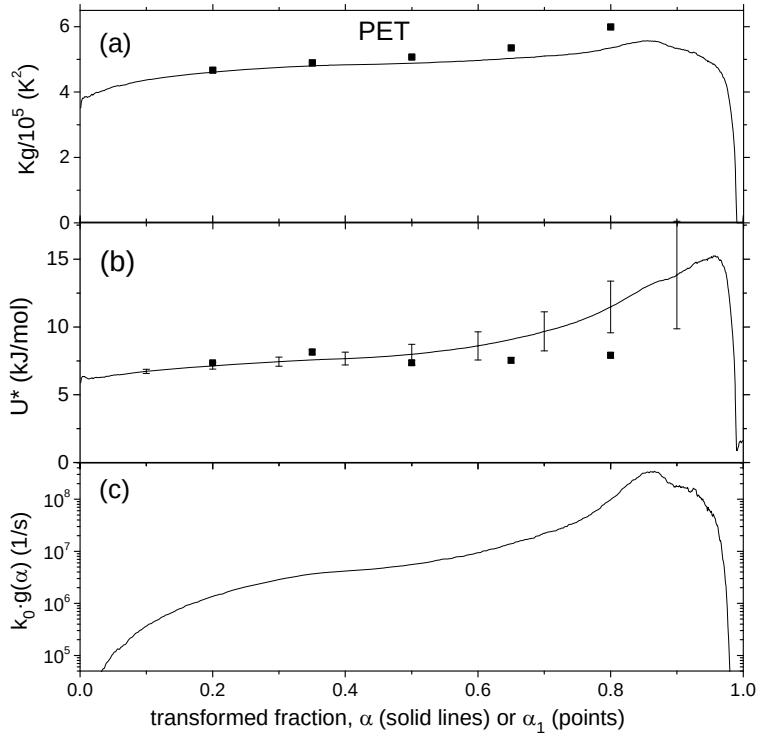

Figure 4.- Dependence of the kinetic parameters of PET crystallization on the transformed fraction. Solid lines and error bars: overall crystallization process. Points: main crystallization process (see main text).

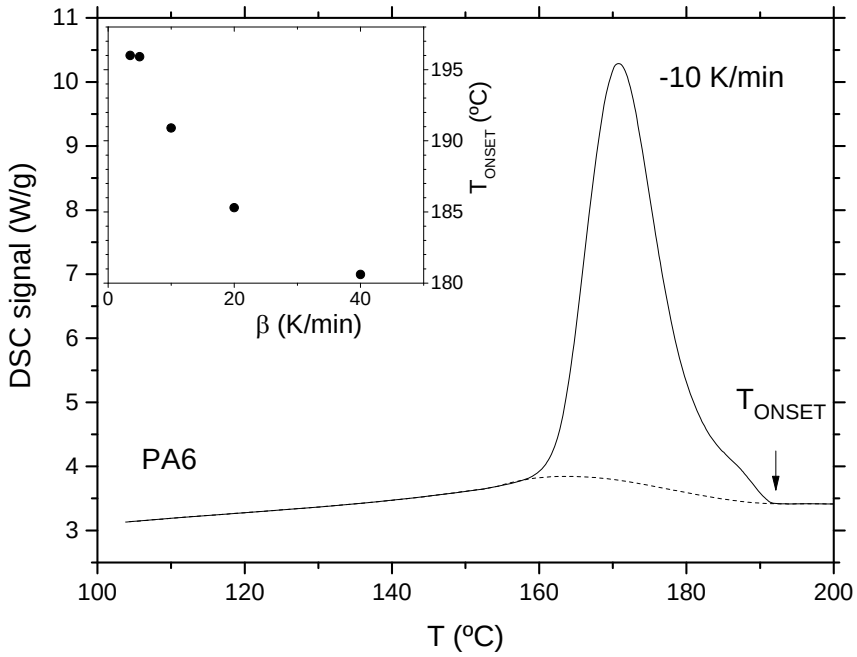

Figure 5.- Deconvolution of the PA6 DSC peaks to subtract the process occurring at long times (dashed line). Inset: onset temperature *vs* heating rate.

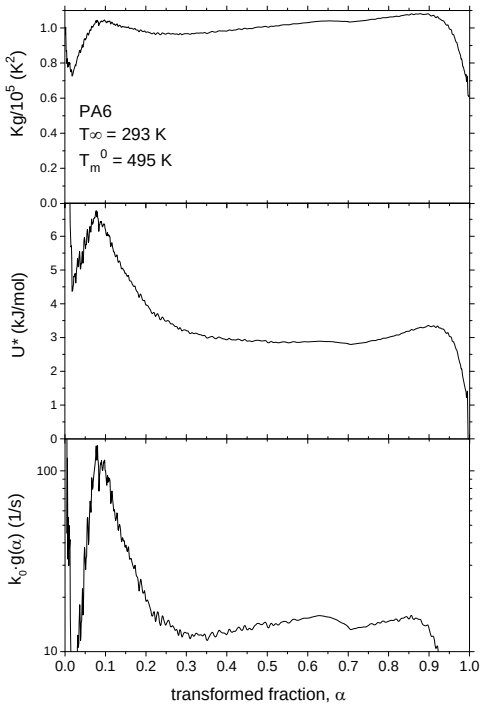

Figure 6.- Kinetic parameters of PA6 obtained from the DSC experiments.

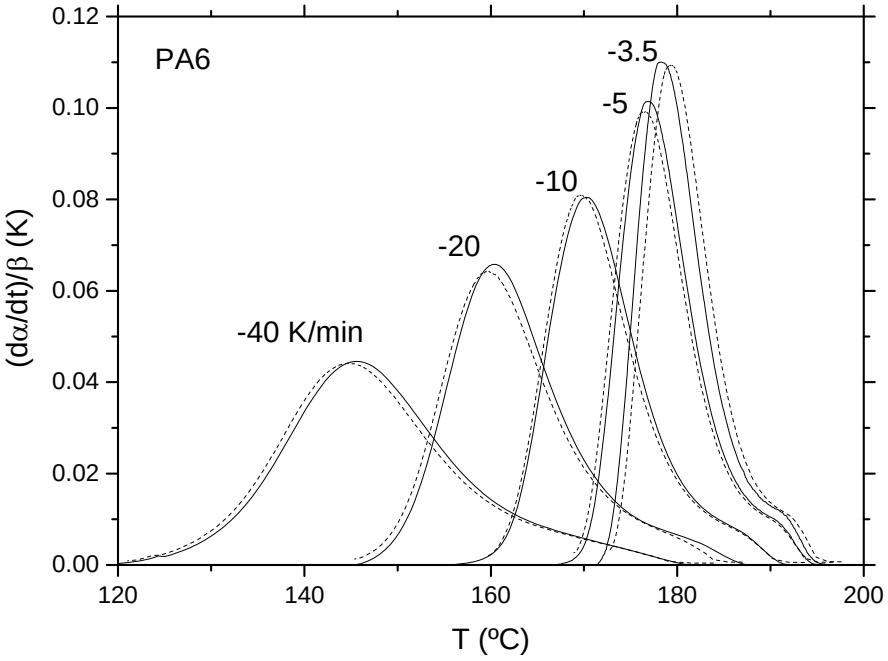

Figure 7.- Transformation rates during melt crystallization of PA6 at several cooling rates: experiment (solid lines), prediction (dashed lines).

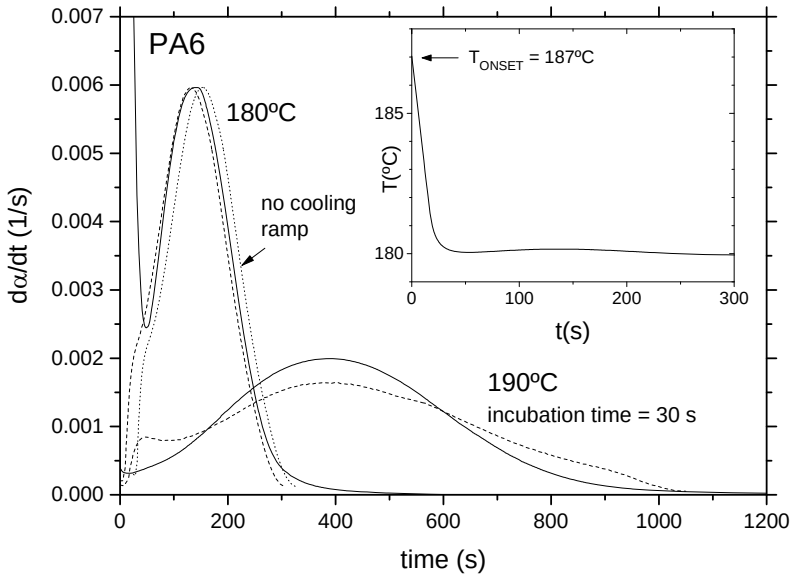

Figure 8.- Crystallization rate of PA6 during two isothermal stages reached at -20 K/min: experimental curves (solid lines), predicted curves (dashed lines). The curve labelled "no cooling ramp" means that crystallization before the isotherm has been neglected. Inset: T(t) dependence before the 180ºC isotherm is reached.

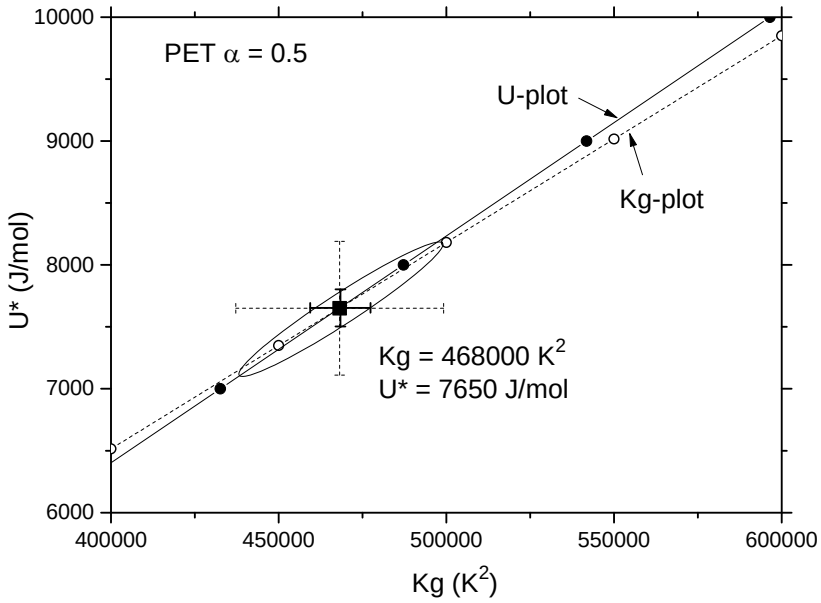

Figure A1.- Correlation between U* and Kg values obtained from the U and Kg plots. Their intersection (filled square) delivers the best fitting values of the H-L dependence of crystallization rate on temperature.

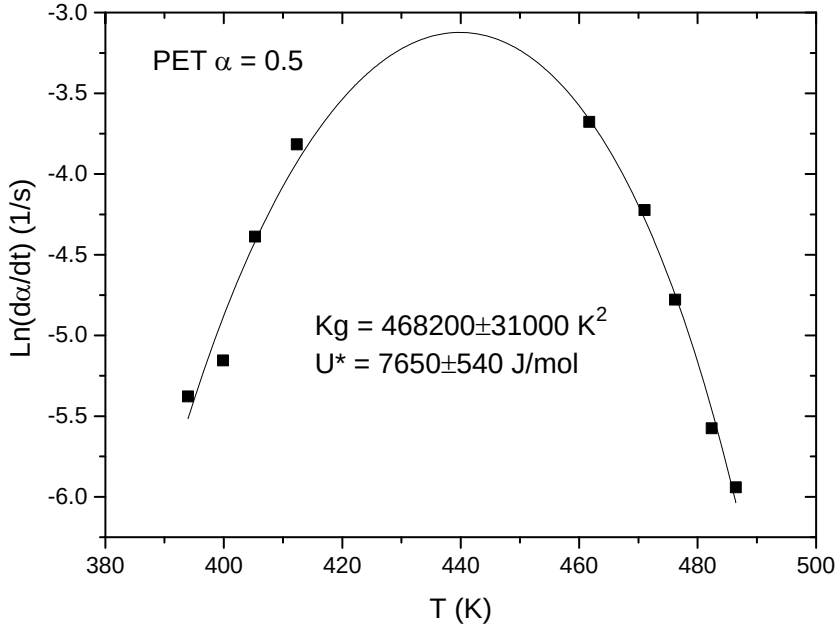

Figure A2.- Non-linear fitting to the H-L crystallization rate dependence on temperature.